IEEE Photonics Journal
An IEEE Photonics Society Publication

Open Access

K-Band Centralized Cost-Effective All-Optical Sensing Signal Distribution Network

Volume 12, Number 6, December 2020

Maged Abdullah Esmail
Amr Ragheb
Hussein Seleem
Habib Fathallah, ***Senior Member, IEEE***
Saleh Alshebeili

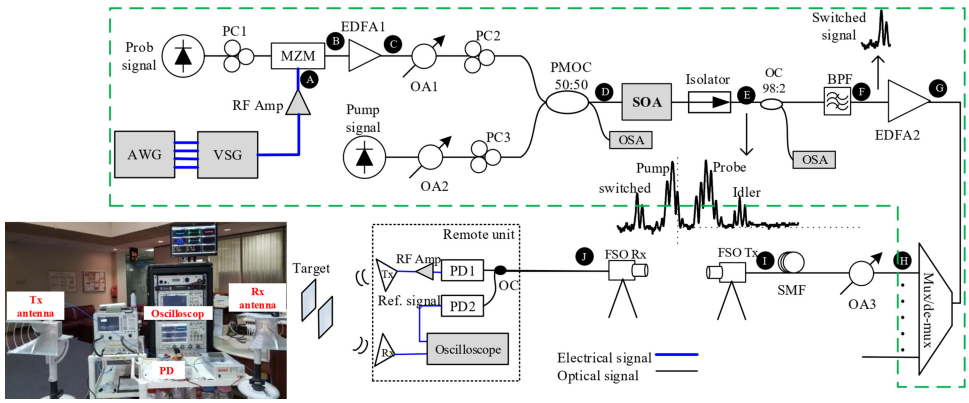

DOI: 10.1109/JPHOT.2020.3034177

K-Band Centralized Cost-Effective All-Optical Sensing Signal Distribution Network

Maged Abdullah Esmail,[1,2] **Amr Ragheb**,[3] **Hussein Seleem**,[4] **Habib Fathallah**,[5] ***Senior Member, IEEE*, and Saleh Alshebeili**[3,6]

[1]Communications and Networks Enginnering Department, Prince Sultan University, Riyadh 11586, Saudi Arabia
[2]Smart Systems Engineering Laboratory, College of Engineering, Prince Sultan University, Riyadh 11586, Saudi Arabia
[3]KACST-TIC in Radio Frequency and Photonics Center (RFTONICS), Riyadh 11421, Saudi Arabia
[4]Department of Electrical Communications and Electronics, Tanta University, Tanta 31527, Egypt
[5]Computer Department of the College of Science of Bizerte, University of Carthage, Tunis 1054, Tunisia
[6]Electrical Engineering Department, King Saud University, Riyadh 11421, Saudi Arabia

DOI:10.1109/JPHOT.2020.3034177

Manuscript received August 17, 2020; revised October 8, 2020; accepted October 24, 2020. Date of publication October 27, 2020; date of current version November 16, 2020. This work was supported by the National Plan for Science, Technology and Innovation (MAARIFAH), King Abdulaziz City for Science and Technology, Kingdom of Saudi Arabia, Award Number 3-17-09-001-0012. Corresponding author: Maged Abdullah Esmail (e-mail: mesmail@psu.edu.sa).

Abstract: In this work, we propose and experimentally demonstrate a centralized all-optical network for sensing signal distribution to a large number of remote sites. The reach range of high-resolution sensing systems is often limited due to atmospheric effects. Employing a centralized optical fiber network for signal distribution to different nodes increases the effective reach distance, decreases the power consumption, and reduces the overall cost of the sensing system. The proposed centralized all-optical network is structured such that it has an all-optical wavelength converter hosted at a central office to guide a sensing signal to a specific site/sensor. This system enables using shared equipment in the transmitter which in turn reduces the overall cost of the network. The performance of the proposed system is investigated by transmitting a radar signal over various transmission media, i.e. fiber, free space optic (FSO), and hybrid fiber/FSO. Some empirical formulas for the signal power and dynamic range (DR) are derived. The results show that although optical signal switching introduces a penalty of 2.5-dB in the signal (DR), the signal still preserves its good shape and spectrum quality. In addition, the experimental results show the system performance with respect to target detection and range estimation.

Index Terms: All-optical network, free-space optics, semiconductor optical amplifier (SOA), sensing signal distribution, wavelength conversion.

1. Introduction

A sensor network is a network that combines arrays of sensor elements which are deployed to perform different tasks such as safety, security, environmental monitoring, etc. Among these sensor networks is radar sensor network which is used for various applications in many fields. In the past,

the development of radar was dedicated to military and security applications, such as air defense, weapon guidance, ship surveillance, and so forth. However, currently, radar sensors are being used for several civilian applications, such as objects detection and positioning, navigation, imaging, mapping, cancer detection, and autonomous vehicle guidance [1]. With the expanding range of radar applications, the need for new spectrum bands leads to the exploitation of high frequencies in the radio frequency (RF) spectrum. Nowadays, radar sensors can operate over various RF bands ranging from a few gigahertz (S-band) to sub-terahertz (infrared band) [2].

Operation at high frequencies in the millimeter-wave (MMW) range and beyond limits the reach distance/coverage area of radar systems to a few hundred meters or less. The outdoor environment can introduce high attenuation in the range of 1-dB/km or more for MMW signals. The attenuation is expected to increase depending on weather conditions. Using fiber cables to distribute radar signals to remote sites is a promising solution to extend radar reach distance and build radar networks. Fiber-based networks have the advantages of low power loss, high immunity to electromagnetic interference, and a large coverage area [3]–[4].

Using fiber optic links for radar signal distribution has been investigated in previous studies. In [5] and [6], an ultra-wideband (UWB) radar signal was generated and converted into an optical signal using a polarization modulator. The optical signal was then transmitted over a 3-km single-mode fiber (SMF). Then, a colorless RF front-end was used to transmit the radar signal and receive the echo. In [7] and [8], a chaotic laser source was used to generate and transmit an 18-GHz bandwidth radar signal over a 24-km SMF for remote water-level measurement and ranging applications. MMW radar signal transmission over a fiber-based network was recently demonstrated in [3]. Moreover, three different radar signals were generated and modulated over three different optical carriers in [4]. Then, a wavelength-division multiplexing (WDM) device was used to direct these signals to RF antenna units. A frequency-modulated continuous-wave (FMCW) radar signal with a 96-GHz RF carrier was transmitted over a 3-km SMF to detect small debris/objects on airport runways. However, no WDM network was considered in this study. Small-drone-detection based on an FMCW radar system was proposed in [9]; the radar's transmitter and receiver are mounted on two separate platforms to reduce power-coupling leakage between them. Then, fiber cable is used as a connection line between the platforms.

In our previous work [10], we analyzed the performance of a semiconductor optical amplifier (SOA) device for radar signal switching, taking into account the radar signal power and RF band (i.e., carrier frequency). Moreover, we investigated the effect of the probe and pump signals' powers and wavelength detuning in the switching setup on the switched signal. Herein, we propose a cost-effective all-optical transport network for radar signal distribution. Instead of dedicating one complete radar system for each site as proposed in previous studies [3]–[6], [9], we consider generating one radar signal in the central office (CO) and then transmitting it over one selectable branch of a point-to-multipoint optical network by exploiting the SOA's wavelength conversion function in the CO as discussed in Section 2. Because of the limitation of hardware availability in our lab, the demonstration and analysis are performed over the downstream link for signal distribution only (see Fig. 1). The upstream setup can be built using out of the shelf components. For N remote sensors, the wavelength converter is controlled to generate sequential wavelengths that carries the sensing signals. These wavelengths are selected to fit one of the WDM ports which are connected to remote sensors by fiber segments. In general, the proposed network provides the following advantages:

1) Centralized generation and analysis of sensing sgianls;
2) Reduced overall cost by sharing the expensive signal generation and processing equipment in the CO. This, in turn, contributes to the compactness and reduced hardware complexity of remote sites;
3) Transparency to the sensing signal bandwidth because no limited-bandwidth electronic switches are employed;
4) Transmission using an OSSB signal with a high suppression ratio, which mitigates the effect of fiber CD;

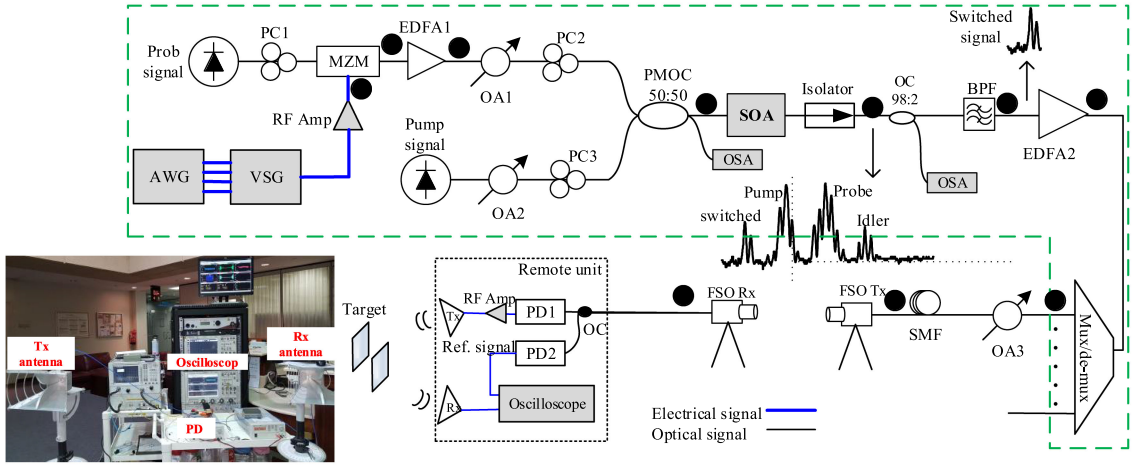

Fig. 1. Experimental setup for radar signal transmission and distribution. AWG: arbitrary waveform generator, VSG: vector signal generator, PC: polarization controller, OA: optical attenuator, MZM: Mach–Zehnder modulator, PMOC: polarization-maintaining optical coupler, SOA: semiconductor optical amplifier, BPF: bandpass filter, EDFA: erbium-doped fiber amplifier, OC: optical coupler, PD: photodetector, SMF: single-mode fiber, FSO: free-space optic, OSA: optical spectrum analyzer. The dashed box in green defines the shared devices among all the remote units/sensors.

5) Employment of all-optical free space optic (FSO) links, which are a good alternative when fiber installation is expensive or impossible.

By controlling the SOA injection current and the optical input power, a ∼20 dB sideband suppression ratio (SSR) is achieved. The experimental results show that using optical single-sideband (OSSB) mitigates the chromatic dispersion (CD). We found that radar signal switching introduced a penalty of 2.5-dB in the radar signal dynamic range (DR). Empirical models for the radar signal DR and power were derived according to the received optical power. Moreover, target detection and ranging were investigated in this work as a proof of concept for this proposed network.

The remainder of the paper is organized as follows. In Section 2, we discuss the all-optical network experimental setup for radar signal distribution. The experimental results are analyzed in Section 3. Finally, we present our conclusions in Section 4.

2. Experimental Setup Description

Our experimental setup, shown in Fig. 1, was used to demonstrate radar signal switching and transmission over an all-optical network. However, it can be used for any type of sensing signals. In this network, the radar signal transmission is performed optically, without the need for optical-to-electrical (OE) and electrical-to-optical (EO) conversion during wavelength switching or transmission over either an SMF or FSO link. The radar signal, as a baseband waveform, is first generated using an arbitrary waveform generator (Keysight AWG M8190 A, with a 12-GSa/s sampling rate). A chirp signal with a pulse width (PW) of 1-μs, a 4-μs pulse-repetition interval (PRI), and a 100-MHz bandwidth is generated. This radar signal is then up-converted to the K-band at a 24-GHz carrier using a vector signal generator (VSG, Keysight PSG E8267D).

Next, the K-band radar signal is amplified using an RF amplifier (SHF 827, with 10-dB gain) and applied to a wideband-intensity Mach–Zehnder modulator (MZM, with a 40-GHz bandwidth) to convert the electrical signal to the optical domain. A direct-current power supply of 7.1-V is used to adjust the operating/biasing point of the modulator. The MZM exploits a laser diode source (Keysight N7714 A) with a wavelength of 1551.7-nm as a probe signal that carries the radar signal. The MZM power loss is compensated by using an erbium-doped fiber amplifier (EDFA1). The output

signal of the EDFA is combined with the pump signal of a laser diode operating at 1550.11-nm. The power combiner is a polarization-maintaining optical coupler (PMOC) with a coupling ratio of 50:50.

The output signal of the PMOC is then injected into a nonlinear SOA (Kamelian SOA-NL-L1-C-FA) device. The nonlinearity of the SOA device makes it suitable for various nonlinear applications, such as four-wave mixing (FWM), self-phase modulation (SPM), and cross-gain modulation (XGM) [11]. The SOA provides high gain recovery (approximately 25-ps) and low polarization dependence (approximately 1-dB). Additionally, it provides a fiber-to-fiber gain of approximately 10-dB. The power level and the polarization of the input signals to the SOA are adjusted using polarization controllers (PCs) and optical attenuators (OAs).

An optical isolator is used at the output of the SOA to prevent back-reflected signals, which can increase the relative noise intensity of the SOA. Since the resulting OSSB-switched signal has low power, a bandpass filter (BPF) with a bandwidth of 2.4-nm centered at 1547.72-nm is used to reject the unwanted signals to the right of the switched signal. This ensures a high amplification ratio for the OSSB signal containing the desired radar signal. The output of EDFA2 is then forwarded to a 1:40 mux/de-mux (100-GHz spacing) where the switched signal can be transmitted over any channel by changing the pump signal wavelength. As the radar signal frequency is 24-GHz, a mux/de-mux with 25-GHz spacing is preferred. However, due to the unavailability of such a device in our laboratory, we used 100-GHz mux/de-mux.

The output signal of the mux/de-mux is then transmitted over various transmission mediums (SMF, FSO, hybrid SMF/FSO). Two SMFs were considered in this experiment—12- and 37-km in length—with signal attenuation of 0.182- and 0.172 dB/km, respectively, at a wavelength of 1550-nm. The FSO segment is an all-optical link consisting of two identical SMF collimators. The lenses of the collimators have full-angle beam divergence of 0.032°, with a 3.6-mm output-beam diameter. The all-optical FSO link is transparent to the fiber, where no OE or EO conversion is required, as in traditional FSO links [13].

In the front-end (i.e. remote site), the FSO link output signal is split by an optical coupler (OC) with a 50:50 splitting ratio to two photodetectors (PDs). The first PD has a 65-GHz bandwidth that beats the OSSB with the carrier to generate the RF radar signal. The generated RF signal is then amplified by an RF amplifier and transmitted over free space using a horn antenna with 13-dBi gain. The echo signal is received by another horn antenna with 13-dBi gain. The received echo signal is then analyzed with a high-speed oscilloscope (Keysight DSO-X 93204 A, with 32-GHz). The other arm of the OC is connected to a 70-GHz PD2 to generate the reference RF signal. Note that the reference signal can also be obtained from PD1's output by using an RF power divider. In addition, an optical spectrum analyzer (Keysight OSA 86142B) with 0.06-nm resolution bandwidth was used to measure and monitor the optical signal spectrum at various points in the experimental setup using optical couplers, as shown in Fig. 1.

3. Experimental Results

In this section, we first discuss the generation of an OSSB signal using an SOA device with a high suppression ratio. Then, we discuss the performance of the transmitted radar signal over the all-optical network. Because of the limitation of hardware availability in our lab, the demonstration and analysis are performed over the downstream link only where we investigate the received echo signals for two arbitrary targets at the remote site.

3.1 Optical Single-Sideband (OSSB) Signal Generation

The SOA device in this work is used to convert the signal wavelength of the original modulated signal to a new desired wavelength that fits a specific port in the mux/de-mux device. This eliminates the need to use electronic switches, which require OE and EO converters that limit the signal bandwidth. By controlling the pump-signal wavelength, the switched signal can be generated to fit any wavelength in the mux/de-mux grid [10]. In addition, an OSSB signal with a high SSR is preferred over a double-sideband (DSB) signal, which reduces the bandwidth consumption.

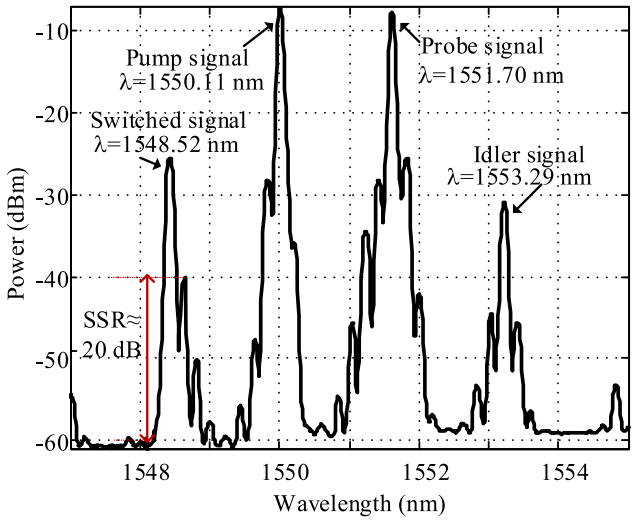

Fig. 2. Power spectrum of the output signal of the SOA. The switched signal at 1548.52-nm has SSR≈ 20 dB.

Moreover, transmitting the SSB signal reduces the CD, which can lead to sideband cancellation at the PD in the case of DSB signal reception [14]. Note that the generation of the OSSB and wavelength conversion in this work are accomplished simultaneously using the same scheme.

To generate an OSSB signal with a high SSR to combact the CD effect, we need to control and optimize the injection current of the SOA and the power of the input signals to the SOA [10]. The input signals to the SOA must have parallel polarization to achieve efficient FWM [12]. This helps to obtain an OSSB switched signal with the maximum suppression ratio. The PCs at the input of the SOA are used to achieve parallel polarization. The SSR is defined as the difference between the first two sidebands around the carrier (see Fig. 2). A maximum SSR of approximately 20-dB is achieved at a 300-mA injection current, which is the typical bias value of the SOA device used. The power values of the probe and pump signals were found to be 0.17- and 4-dBm, respectively. Based on these values, Fig. 2 presents the output signal of the SOA. This figure shows the effect of the FWM; two additional waves beside the probe signal and the pump signal are created. These are the switched signal at 1548.52-nm and the idler signal at 1553.29-nm. Note that the PD in the RF front-end, which is used to convert the optical signal into an electrical signal, needs to beat the carrier signal and the upper sideband signal to regenerate the radar signal.

3.2 Performance of Radar Signal Over All-Optical Network

In this section, we consider three configurations for the transmission medium: SMF, FSO, and hybrid SMF/FSO. FSO is useful when fiber installation is impossible or expensive, e.g., when there are rivers, highways, mountains, private properties, and so forth. In border surveillance and other tactical applications, FSO is always preferred over fiber because of fast installation and configuration time, ad-hoc and short time installation, digging avoidance, and so forth. In our experimental setup, to be able to use the standard 100-GHz mux/de-mux device, we selected the wavelengths of the pump and probe signals so that the generated switched signal wavelength would fit a specific channel of the ITU dense wavelength-division multiplexing (DWDM) grid. Table 1 lists some possible switched signal wavelengths, which are achieved by controlling the pump-signal wavelength. In this study, we fixed the probe signal wavelength at 1551.7-nm. The wavelength of the pump signal changes, as listed in Table 1. We examined the performance of the radar signal at the output of three DWDM channels (Ch#36, Ch#37, Ch#38), as shown in Table 1. The DR of the radar signal is considered as a performance metric. Signal DR is defined as the ratio of the

TABLE I
Some Switched Signal Wavelength Values That Correspond to ITU-DWDM Grid Standard

Ch#	Pump signal wavelength	Switched signal wavelength
35	1550.51 nm	1549.32 nm
36	1550.11 nm	1548.52 nm
37	1549.71 nm	1547.72 nm
38	1549.31 nm	1546.92 nm
39	1548.91 nm	1546.12 nm

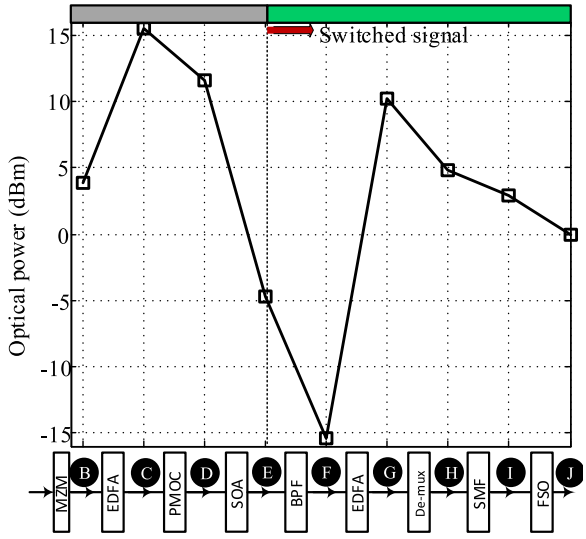

Fig. 3. Power budget of the all-optical transmission system. The letters show the measurement points in the setup (see Fig. 1).

highest signal power to the lowest signal power. We noticed a negligible change in the radar signal DR after mux/de-mux for the three channels with DR$\approx 33 \pm 0.2$ dB.

The optical power budget of the transmission system is shown in Fig. 3. Because of the low power of the switched signal, an EDFA is placed in cascade to the BPF. The 12-km SMF introduces approximately 2-dB power loss, while the FSO channel introduces approximately 3-dB power loss. Assuming that the laser beam has a Gaussian power distribution, the theoretical geometrical loss of the FSO link is approximately 0.5-dB. The remaining power loss is due to link misalignment and light collimation to the SMF.

The power spectra of the radar signal obtained at various points in our experiment are compared in Fig. 4. The radar signal generated by the VSG has a DR of 50-dB. The EO conversion via MZM introduces a 13-dB drop in the signal DR. After wavelength conversion by the SOA and channel selection via mux/de-mux, the DR device incurs only a 2.5-dB penalty. The 12-km SMF introduces a 2-dB drop in the DR. Finally, a 3-dB drop in the radar signal DR is introduced by the FSO link. These results indicate that most of the signal DR penalty is introduced by conversion of the electrical signal into an optical signal using the optical modulator. The process of radar signal switching in the network (i.e., wavelength conversion and channel selection) has little effect. Moreover, the curves in Fig. 4 show that, despite the penalty in the signal DR, the signal maintains good quality in comparison to the signal generated by the source. This is clear from the insets of the time-domain signals shown in Fig. 4 where, although the received signal, after the FSO link, has the lowest DR of ~ 30 dB, it still exhibits a similar shape to the signal generated by the VSG.

The effect of the optical received power at the PD input on the DR and the RF power of the radar signal are presented in Fig. 5. Fig. 5(a) shows the effect of the optical received power

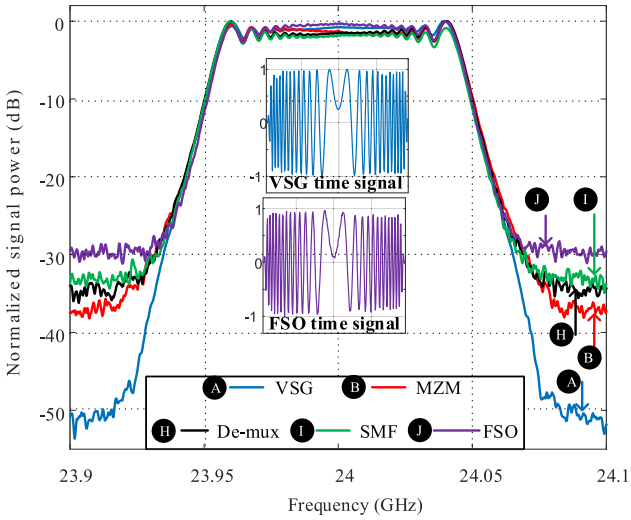

Fig. 4. Radar signal normalized power spectrum vs. frequency at various points in the transmission system. The letters show the measurement points in the setup (see Fig. 1).

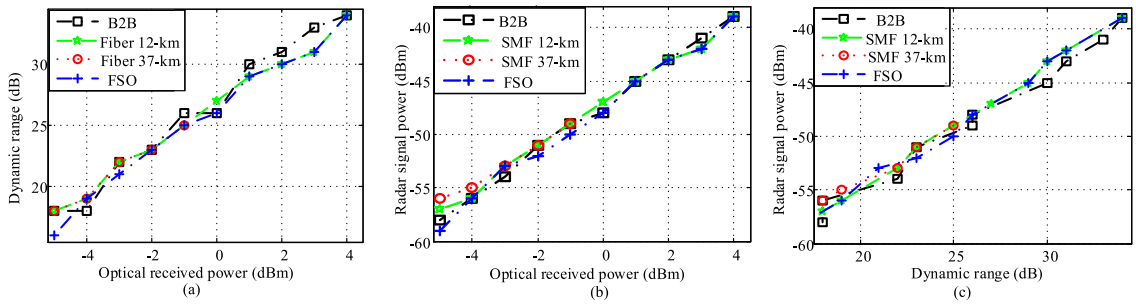

Fig. 5. (a) Radar signal dynamic range vs. optical received power, (b) radar signal power vs. optical received power, and (c) radar signal power vs. dynamic range.

(at the PD input) on the DR of the radar signal (at the PD output) through various transmission mediums: a 12-km SMF, a 37-km SMF, a 6-m FSO channel, and back-to-back (B2B) without a transmission medium. The curves show that transmitting the radar signal over different channels has a negligible effect on the signal DR. Moreover, it shows that increasing the optical transmitted power can improve the signal DR. This improvement appears linear (in dB–dB scale) and can be approximated by the following empirical equation:

$$DR(dB) = 1.834 P_r(dBm) + 26.71, \tag{1}$$

where P_r is the optical received signal power (in dBm), and DR is the output radar signal DR (in dB). The coefficient (1.834) and constant (26.71) are obtained using data fitting to better predict DR values. Equation (1) can be considered as a hybrid RF-optic (RO) equation because it links the optical power measurement to an RF counterpart. This type of empirical hybrid equation is becoming increasingly important for emerging applications that involve hybrid RO technologies. Using (1), the root-mean-square error (RMSE) and R-squared goodness of fit were found to be (0.87, 0.98), (0.54, 0.99), (0.45, 0.97), and (0.70, 0.98) for B2B, the 12-km SMF, the 37-km SMF, and the 6-m FSO channel, respectively. The small values of RMSE and the high goodness of fit close to one reflect the accuracy of (1) to predict the RF signal DR when the optical received signal power is identified.

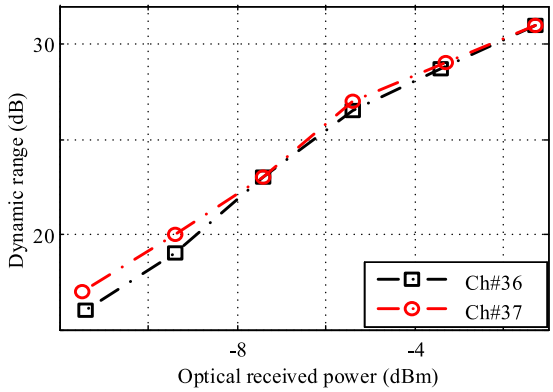

Fig. 6. Echo signal performance at two different optical channels of the proposed network.

In Fig. 5(b), the effect of the optical received signal power on the improvement of the radar signal power is presented. The radar signal power improves with increasing optical received signal power. For instance, for an optical received power of 0-dBm, the received radar signal power is approximately -47 dBm. If the received optical power is increased by 4-dB, the radar signal power improves by approximately 8-dB. The linear relationship between the received optical power at the PD input and the resultant radar signal power at the PD output can be calculated using the derived empirical formula below:

$$P_{RF}(dB) = 2.041 P_r(dBm) - 47.31. \tag{2}$$

The results of the RMSE and the R-squared goodness of fit test are (0.42, 0.99), (0.44, 0.99), (0.78, 0.91), and (0.69, 0.99) for B2B, the 12-km SMF, the 37-km SMF, and the 6-m FSO channel, respectively. Equation (2) is also a hybrid RO equation bringing the RF and optical powers together in an empirical relationship.

Finally, we investigate the relationship between the radar signal DR and its power at the PD output. The results in Fig. 5(c) show a linear relationship between them. According to (1) and (2), this relationship is described by the following formula:

$$P_{RF}(dB) = 1.1 DR(dB) - 77.03. \tag{3}$$

The DR improves by 0.9-dB as the received radar signal power increases by 1 dB.

3.3 Remote Target Detection and Ranging

In this section, we investigate the performance of the proposed centralized network for remote target detection and ranging, for applications including objects on railways, runways, and so forth. Fig. 1 shows the design of the remote antenna unit for this application and some equipment used in this setup.

Fig. 6 shows a comparison of the echo signal performance in terms of the signal DR versus the received optical power for Ch#36 and Ch#37 listed in Table 1. The two channels achieve almost the same performance. To examine the capability of the system for object detection and ranging, we put two metal targets at 5.5-m and 9.5-m away from the RF front-end. The two antennas were facing the same direction. In addition, they were positioned 1.6-m above ground with 1.1-m spacing to reduce power leakage from the transmitter to the receiver. A system delay $\approx$22-ns, including RF cables and fiber cable delays after the OC in the RF frontend, was measured. This delay value was used to calibrate the range of the target. By performing cross-correlation between the echo signal and the reference signal, we obtained the two peaks shown in Fig. 7. The first peak at 58.6-ns in Fig. 7 corresponds to the first target, and the second peak at 85-ns corresponds to the second target. By subtracting the system delay from the round trip time, the estimated locations were

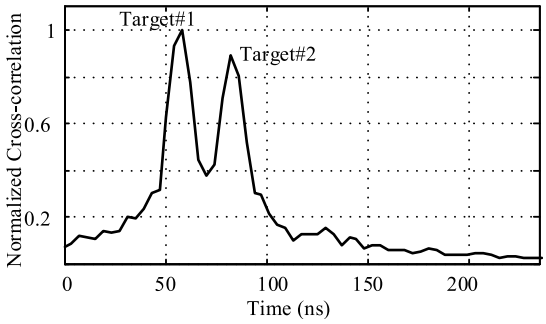

Fig. 7. Target detection and ranging using the proposed network.

determined to be 5.48-m and 9.45-m for the first and second targets, respectively. Compared with the actual locations, range errors of 0.01-m and 0.05-m were found for the first target and second target, respectively.

4. Conclusion

We experimentally investigated the capability of an all-optical network to transport radar signal over hybrid SMF/FSO links. An SOA is employed to generate an OSSB signal with an SSR of approximately 20-dB. The effect of radar signal switching and transmission was studied with respect to the radar signal power and DR. The DR penalty incurred due to radar signal switching (i.e., wavelength conversion and channel selection) is 2.5-dB. Moreover, we observed a slight variation in the radar signal DR at the mux/de-mux output ports in the range of $\pm$0.2 dB. Investigating the effect of radar signal transmission over the OSSB signal and over various transmission links (12-km SMF, 37-km SMF, and 6-m FSO) revealed a negligible change in the radar signal DR and the power at the PD output for the same optical received power at the PD input. The DR and power of the radar signal vary almost linearly with respect to the optical signal power. Empirical models for the radar signal DR and power were derived. As a proof of concept, we investigated the capability of this network to perform remote target ranging and detection. The results showed negligible change in echo signal performance over two different optical channels of the network. The system was able to detect two targets simultaneously with a range error smaller than 0.05-m.

References

[1] S. M. Patole, M. Torlak, D. Wang, and M. Ali, "Automotive radars: A review of signal processing techniques," *IEEE Signal Process. Mag.*, vol. 34, no. 2, pp. 22–35, Mar. 2017.
[2] B. Zhang, Y. Pi, and J. Li, "Terahertz imaging radar with inverse aperture synthesis techniques: System structure, signal processing, and experiment results," *IEEE Sensors J.*, vol. 15, no. 1, pp. 290–299, Jan. 2015.
[3] S. Futatsumori, K. Morioka, A. Kohmura, K. Okada, and N. Yonemoto, "Design and field feasibility evaluation of distributed-type 96 GHz FMCW millimeter-wave radar based on radio-over-fiber and optical frequency multiplier," *J. Lightw. Technol.*, vol. 34, no. 20, pp. 4835–4843, Oct. 2016.
[4] A. Kanno, T. Kuri, and T. Kawanishi, "Optical-network-connected multi-channel 96-GHz-band distributed radar system," in *Proc. SPIE 9462*, 2015, pp. 94620A–94620A-9.
[5] J. Zheng, H. Wang, J. Liu, N. Zhu, J. Fu, and S. Pan, "Fiber-optic remote Ultra-wideband noise radar with colorless base station," in *Proc. IEEE Int. Topical Meeting Microw. Photon.*, 2013, pp. 134–137.
[6] J. Zheng *et al.*, "Fiber-distributed Ultra-wideband noise radar with steerable power spectrum and colorless base station," *Opt. Express*, vol. 22, no. 5, pp. 4896–4907, 2014.
[7] Y. Ji *et al.*, "Microwave-photonic sensor for remote water-level monitoring based on chaotic laser," *Int. J. Bifurcation Chaos*, vol. 24, no. 3, 2014, Art. no. 1450032.
[8] M. Zhang, Y. Ji, Y. Zhang, Y. Wu, H. Xu, and W. Xu, "Remote radar based on chaos generation and radio over fiber," *IEEE Photon. J.*, vol. 6, no. 5, Oct. 2014, Art no. 7902412.
[9] D. H. Shin, D. H. Jung, D. C. Kim, J. W. Ham, and S. O. Park, "A distributed FMCW radar system based on fiber-optic links for small drone detection," *IEEE Trans. Instrum. Meas.*, vol. 66, no. 2, pp. 340–347, Feb. 2017.
[10] M. A. Esmail, A. M. Ragheb, H. Fathallah, and S. A. Alshebeili, "Radar signal transmission and switching over optical networks," *Opt. Commun.*, vol. 410, no. 1, pp. 385–388, 2018.

[11] F. Saadaoui, M. Fathallah, A. M. Ragheb, M. I. Memon, H. Fathallah, and S. A. Alshebeili, "Optimizing OSSB generation using semiconductor optical amplifier (SOA) for 5G millimeter wave switching," *IEEE Access*, vol. 5, pp. 6715–6723, 2017.
[12] G. Contestabile, L. Banchi, M. Presi, and E. Ciaramella, "Investigation of transparency of FWM in SOA to advanced modulation formats involving intensity, phase, and polarization multiplexing," *J. Lightw. Technol.*, vol. 27, no. 19, pp. 4256–4261, Oct. 2009.
[13] M. A. Esmail, A. Ragheb, H. Fathallah, and M. S. Alouini, "Investigation and demonstration of high speed full-optical hybrid FSO/Fiber communication system under light sand storm condition," *IEEE Photon. J.*, vol. 9, no. 1, Feb. 2017, Art. no. 7900612.
[14] G. H. Smith, D. Novak, and Z. Ahmed, "Overcoming chromatic-dispersion effects in fiber-wireless systems incorporating external modulators," *IEEE Trans. Microw. Theory Tech.*, vol. 45, no. 8, pp. 1410–1415, Aug. 1997.